POLYPUBLIE
Polytechnique Montréal

POLYTECHNIQUE MONTRÉAL
UNIVERSITÉ D'INGÉNIERIE

Titre: Crossflow microsand filtration in cooling tower systems to control fouling in heat exchanger devices
Title:

Auteurs: Vaishali Ashok, Faezeh Absalan, Alain Silverwood, Étienne Robert, Dominique Claveau-Mallet, & Émilie Bédard
Authors:

Date: 2024

Type: Article de revue / Article

Référence: Ashok, V., Absalan, F., Silverwood, A., Robert, É., Claveau-Mallet, D., & Bédard, É. (2024). Crossflow microsand filtration in cooling tower systems to control fouling in heat exchanger devices. Journal of Building Engineering, 95, 110167 (11 pages). https://doi.org/10.1016/j.jobe.2024.110167
Citation:

Document en libre accès dans PolyPublie
Open Access document in PolyPublie

URL de PolyPublie: https://publications.polymtl.ca/58888/
PolyPublie URL:

Version: Version officielle de l'éditeur / Published version
Révisé par les pairs / Refereed

Conditions d'utilisation: Creative Commons Attribution 4.0 International (CC BY)
Terms of Use:

Document publié chez l'éditeur officiel
Document issued by the official publisher

Titre de la revue: Journal of Building Engineering (vol. 95)
Journal Title:

Maison d'édition: Elsevier
Publisher:

URL officiel: https://doi.org/10.1016/j.jobe.2024.110167
Official URL:

Mention légale: © 2024 The Authors. Published by Elsevier Ltd. This is an open access article under the CC BY license (http://creativecommons.org/licenses/by/4.0/).
Legal notice:

Ce fichier a été téléchargé à partir de PolyPublie, le dépôt institutionnel de Polytechnique Montréal
This file has been downloaded from PolyPublie, the institutional repository of Polytechnique Montréal

https://publications.polymtl.ca

Journal of Building Engineering 95 (2024) 110167

Contents lists available at ScienceDirect

Journal of Building Engineering

journal homepage: www.elsevier.com/locate/jobe

Crossflow microsand filtration in cooling tower systems to control fouling in heat exchanger devices

Vaishali Ashok [a], Faezeh Absalan [a], Alain Silverwood [b], Etienne Robert [c], Dominique Claveau-Mallet [a], Emilie Bédard [a,*]

[a] Civil Geological and Mining Engineering Department, Polytechnique, Montreal, Canada
[b] Xylem Water Solutions and Water Technology, Washington DC, USA
[c] Mechanical Engineering Department, Polytechnique, Montreal, Canada

ARTICLE INFO

Keywords:
Side stream filtration
Building energy
HVAC
Clogging

ABSTRACT

In the context of global warming, there is a growing need for high-performance heat, ventilation and air conditioning systems. Fouling is a challenge, affecting heat exchanger operational and energetic performance. Side stream filtration can be used to improve water quality by reducing particle concentration in the system. The aim of this study was to assess a crossflow microsand filtration unit's efficacy in reducing fouling within an 81-plate heat exchanger, in an in-situ cooling tower circuit. A pilot heat exchanger without filtration was operated under similar conditions. After 3 years of continuous operation, visual inspection of the full-scale heat exchanger plates operating with filtration showed minimal accumulation. Pairs of facing plates (7) were scraped and rinsed to collect total solids accumulated on surfaces. Samples were resuspended and analyzed for solids and metal concentration measurements. Low average values of total volatile solids (45 $\mu g/cm^2$) and total solids (93 $\mu g/cm^2$) were indicative of a low biofilm formation. X-ray diffraction revealed the presence of calcite associated to water hardness. Low levels of iron and copper were detected despite slightly corrosive water. In contrast, the pilot heat exchanger exhibited higher deposit accumulation of total volatile solids (90 $\mu g/cm^2$) and total solids (110 $\mu g/cm^2$) after only 12 weeks of operation. These findings underscore the role of side stream filtration in reducing particle deposition and biofouling potential in full-scale cooling tower systems. Crossflow microsand filtration is a promising avenue to control fouling in building cooling tower systems, which could contribute in improving the building's energetic performance.

1. Introduction

With the increase in global cooling demand, the heating ventilation and air conditioning (HVAC) industries are urged to improve their systems' efficiency [1]. Fouling is an undesirable yet common phenomenon in HVAC system heat exchangers (HX). Over the last 40 years, more than 7900 patents were filed on biofouling in heat exchangers according to the Canadian Patent Database [2]. This suggests a recurring problem that has yet to be solved. HX are highly susceptible to fouling due to their high surface area. Fouling in heat exchanger system are of four major types: scaling, corrosion, particulate fouling and biological growth [3]. Scaling is caused by the deposition of inorganic salt in the water circuit. Infeed water, cooling tower (CT) exposed to the atmosphere, chemical additives

* Corresponding author.
E-mail address: emilie.bedard@polymtl.ca (E. Bédard).

https://doi.org/10.1016/j.jobe.2024.110167
Received 6 April 2024; Received in revised form 15 June 2024; Accepted 6 July 2024
Available online 8 July 2024
2352-7102/© 2024 The Authors. Published by Elsevier Ltd. This is an open access article under the CC BY license (http://creativecommons.org/licenses/by/4.0/).

Table 1
Results from selected studies on HX corrosion and fouling with various heat exchange material, circulation fluid, flow and bacterial inoculation.

Material	Fluid and additives	Bacterial inoculation	Lab/on-site	Study duration	Polysaccharide conc./ TSS conc.	Results	Author, Year
Mild steel (MS) coupon	Stagnant Mueller Hinton Broth (MHB) with organic corrosion inhibitors	*CT bacteria Pseudomonas stutzeri*	Laboratory	3 weeks	–	Deep pitting corrosion, corrosion rate 0.047–1.999 mm/y	[12]
Carbon steel (Q235)	Stagnant Postgate C medium	*Desulfovibrio bizertensis*	Laboratory	15 days	Evidence of polysaccharide existence with no measurement of the concentration.	Pitting corrosion with pits depth approaching 15.7 μm. The corrosion rate after 30 days of immersion was (89.9 ± 7.1 μm/y).	[7]
Copper CW024A coupon	Stagnant CT water (1 % chloride) With 2-mercaptopyridine (2-MCP) corrosion inhibitor incubated at 37 °C.	*Bacillus thuringiensis EN2* and *B. oleronius EN9*	Laboratory	14 days		Pitting corrosion rate was 0.025 mm/y for EN2 and 0.036 mm/y for EN9 (control system corrosion rate: 0.004 mm/y).	[19]
P110 steel coupon	Stagnant 3.5 wt% NaCl solution with carbon dioxide (Solution pH = 4) with guar gumgrafted methyl methascrylate (GG-MMA) incubated at 50 °C	No	Laboratory	6 h		Corrosion rate without inhibitor was 26.75 mm/y which reduced to 2.67–8.02 mm/y under various GG-MMA concentrations. Corrosion rate reduced to 0.85 mm/y in the presence of KI (5 mM) + GG-MMA (300 mg/L). GG-MMA is a cathodic type corrosion inhibitor.	[33]
SS316L	Distilled water with sodium bicarbonate, and sodium chloride with Zr coating. Flow rate: 0.5 Lpm- 4 Lpm; Test temperature: 40 °C–65 °C;	No	Laboratory	72 h		Zr coating on the surface declined the formation of fouling deposition rate and increased heat transfer.	[5]
Galvanized steel coupon	Recirculating lab-based cooling tower water Flow: 40 L/min; Test temperature: 28 °C;	No	Laboratory	10 months	The carbohydrate concentration increased to 85.40 ± 3.10 μg/cm^2 during the first 3 months. After that, it increased and decreased until the 10th month. The carbohydrates concentration positively correlated with the weight loss of coupons.	Corrosion rate decreased with time. The corrosion rate after 10 months was 2.41 mg/dm^2 day.	[11]
Mild steel coupon	Stagnant 1 M HCl solution with variation in corrosion inhibitor *Apostichopus japonicus* (AJPS) Test temperature: 25 °C;	No	Laboratory	10 h	Polysaccharide AJPS acted as a strong inhibitor for mild steel corrosion	The 96 % inhibition performance of AJPS was optimized by factorial experimental designs and was found good inhibitor for the protection of mild steel in 1 M HCl.	[34]
Galvanized steel and polymer tubes	Synthetic media comprised of calcium carbonate, magnesium sulfate, sodium chloride, iron oxide, and kaolinite. Flow: 0.8–1.32 gpm; Test temperature: 20–100 °C;	No	Laboratory	108 days		Sticking probability of polymer tube is double than galvanized steel. However, deposit bond strength for galvanized steel is 3 times higher than polymer tube.	[35]
9 copper tubes	CT water (428–7971 mg/L of TDS) with no added chlorine; Velocity 0.9–2.4 m/s;	No	Pilot	86–143 days	Maximum dry matter concentration during the test was 2700 mg/L.	Enhanced tubes showed higher heat transfer performance, compared to the plain tubes.	[13]

(*continued on next page*)

Table 1 (*continued*)

Material	Fluid and additives	Bacterial inoculation	Lab/on-site	Study duration	Polysacharide conc./ TSS conc.	Results	Author, Year
	Temperature of inlet and outlet water: 29.5 and 34 °C respectively;					A pitch to rib height of 13 is recommended for medium fouling potential at a velocity of 0.9–2.4 m/s, targeting inhibition of fouling development.	
Laboratory scale single plate HX with PVC modules	Counter-flow tap water supplemented with nutrients with no added chlorine; Flow rate: 0.047–0.05 gpm Temperature variation: 20–27 °C;	No	Laboratory scale	40 days	Polysaccharides comprise 5–13 % of total EPS 140.4–365.04 μg/cm^2	The heated plates showed lower production of polysaccharides compared to the reference plates (20.0 ± 1.4 °C).	[26]
Stainless steel 10-plate HX (Alfa Laval A45-FG)	Sea water was pumped into the flow-through system (chlorinated on every alternate plate); Velocity: 0.6 m/s; Temperature variation: 27.1–27.4 °C; chlorine residual 1.2 mg/L applied in 2h intervals.	No	Laboratory scale	96 h (4 days)	A maximum of 3 mg/L of combustible matter and 4.5 mg/L of biofilm solids were observed.	Chlorination was effective in controlling the sessile bacterial population during the initial stage of biofilm formation (up to 24 h). Chlorinated plates also exhibited reduced biofilm thickness.	[15]
Stainless steel counter flow HX	Counter-flow system with un-chlorinated artificial hard water containing salts of Ca^{2+}, Mg^{2+}, and $NaHCO_3$. Flow rate: 4.4 gpm; Temperature of cold and hot stream: 33 and 90 °C respectively;	No	Laboratory	12 h		Alternating electromagnetic field could reduce the growth rate of $CaCO_3$ (reduce scaling) and Mg could decrease the $CaCO_3$ crystal particle size.	[4]

such anti-scalants, anti-corrosive agents, biocides, and alkaline agents are some of the factors affecting particle deposition inside the circuit (Kavitha et al., 2019). The scales limit effective heat transfer by insulating the surface exposed to the water [4]. Particulate and biological fouling can also lead to significant heat conductivity reduction [5]. The heat conductivity of stainless steel plates with biofilm reduced from 15 to 0.6 W/m.K, resulting in a 96 % reduction in heat transfer [6]. Corrosion, on the other hand, reduces the mechanical strength of the metal [7].

Defining actions and procedures that better prevent fouling and enhance system's performance over time is critical in the actual climate context. Fouling can be reduced through mechanical cleaning, chemical cleaning, chemical additions, or regular use of side stream filtration units [8]. A range of industrial side-stream filtration technologies are available, such as bag and cartridge, microsand, screen, media and centrifugal separators [9,10]. The primary role of side stream filtration is to continuously filter a portion of water from the CT system to remove suspended solids, silt particles and organics from the mainstream to reduce fouling. Indirect benefits from the process could be higher heat transfer due to cleaner surfaces, lower chemical use, lower maintenance costs and higher energy efficiency of the system [10]. As a result, successful reduction of fouling with side-stream filtration would provide a more sustainable alternative to current cooling tower operating schemes relying heavily on chemical additions to control fouling.

An extensive literature review was conducted on studies reporting HX fouling at pilot scale, either on metal coupons or lab based HXs with simulated operating conditions and the results are summarized in Table 1. Some studies have estimated corrosion, fouling and scaling with simulated CT water [11] and some extracted microorganisms from CT water in an enriched media to test its corrosion, scaling and fouling impact [12]. Gao et al. [13] investigated the deposition behavior of combined fouling by conducting three sets of continuous long-term fouling tests on eight tubes. The study emphasized the role of higher water velocity in reducing the duration of the initial fouling period which occurs prior to the deposition and stabilization periods. In addition, some studies investigated various control measures to reduce fouling. Pinel et al. [14] found that heated modules resulted in reduced extracellular polymer generation associated with biofilm growth when compared to non-heated modules, at pilot plate HX. Also, Murthy et al. [15] found intermittent and continuous chlorination to significantly reduce biofilm thickness. The installation of a biofiltration unit in an open cooling tower system improved recirculation water quality and reduced biofouling compared to a reference installation [16]. The use of more advanced filtrations systems such as ultra and nanofiltration have been reported to treat cooling water make up water, either for reuse of the purge water [17] or to reduce the nutrient and microorganisms content in make up water [18].

Based on the available literature, there are some knowledge gaps that need to be addressed. First, such accelerated biofouling tests using simulated harsher-than-actual water conditions do not truly reflect the fouling and depositions in full scale systems [13]. Second, there is a strong focus on corrosion in these studies, which is only part of the fouling problem [12,19]. Third, the impact of control

measures such as side stream filtration on HX fouling is poorly documented. Finally, there is no reporting of quantitative data on HX fouling at industrial scale. A recent review paper published by Kapustenko et al. [20], mentions a summary of past research work on HX, confirming absence of long term direct measurement studies on fouling of industrial HX of any type. Most types of industrial HX either cannot be dismantled (fused) or are difficult to access (tubular), making it impossible to observe or sample the internal surfaces directly. Even when surfaces are accessible through dismantling, sampling is expensive, and time-consuming.

The aim of this study is to compare fouling characteristics in a heat exchanger under two distinct conditions: with and without the implementation of side-stream filtration. The first system is a heat exchanger integrated into the cooling tower circuit of a full-scale HVAC system. The second system involves a pilot-scale heat exchanger operating with cooling tower water samples derived from the full-scale system but without the application of filtration. The pilot study was necessary due to the challenges associated with disconnecting the filtration unit in an industrial setting. The results thus obtained will help fill in the knowledge gap about the significance of side-stream filtration in preventing fouling, providing valuable knowledge for optimizing HVAC systems, reducing maintenance costs, and increasing overall operational efficiency.

2. Material and methods

2.1. Hospital building study site

The study was performed on a HVAC circuit located in a hospital building in the province of Québec, Canada. This circuit is mainly used for cooling from March to October and heating from November to February. The circuit comprised of 3 cooling towers, 2 heat exchangers, 1 chiller, a basin, and a side-stream filtration unit, as illustrated in Fig. 1. The water was withdrawn from the basin with a 1300 gpm pump and fed to a HX with a total wetted surface of 46.8 m^2. The heated water from the HX then flows through the cooling tower for heat dissipation before returning to the basin. A portion of water is continuously taken out from the basin, filtered, and returned to the basin. The industrial filter was backwashed with municipal water for 8 min every 24 h. Based on the redox potential and chlorine concentrations in the basin water, chlorine-based disinfectants and anti-scaling agents were added through chemical dosing stations. Once the water reached a set upper conductivity level, a volume of water was purged from the system. Municipal water was used as make up and added directly to the basin to compensate for losses due to evaporation and purge. The water temperature in the system was measured every 5 min using the building management system with an accuracy of 0.1 °C. Specifications of the heat exchanger are mentioned in Table 1S.

The side stream filtration unit is a Vortisand® crossflow microsand filtration unit (CMF), (Sonitec-Vortisand inc, Montréal, Canada) installed in 2009. The industrial CMF system operates continuously throughout the day with a steady pumping rate of 45 m^3/h. A daily backwash is performed for 8 min at a flow rate of 189 L per minute. The system has an estimated 3 m^2 footprint and annual maintenance is recommended.

2.2. Sampling of the study site plate heat exchanger

The HX had not been opened and cleaned for the past three years. Water quality in the CT circuit was monitored at the system purge starting on April 12th, 2022. Mean values for physico-chemical parameters are presented in supplemental material (Table 2S). The side stream filtration unit was running continuously until March 6th, 2023, at which time it was stopped to start the study period without

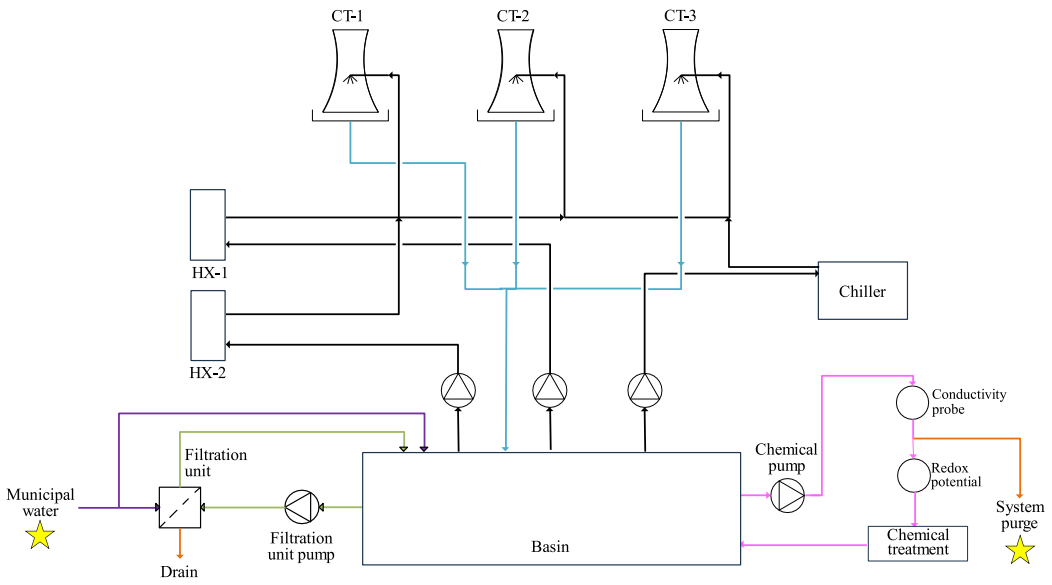

Fig. 1. Schematic of the on-site heat exchanger circuit. The sampling points are indicated with a star.

side filtration. The HX cleaning and sampling was initially planned concurrently with the shutdown of the side stream filtration system. However, delays were experienced and the HX cleaning occurred 7 weeks after the side stream filtration was shutdown. During this period between side filtration shutdown and HX sampling, the outside temperatures were not high enough to require the use of the HX and of the cooling towers. On May 23rd, the HX was stopped and opened for sampling (Fig. 2A). In total, 14 plates out of 81 (17 %) were sampled (Fig. 2B) with an equivalent surface area of 8.1 m^2. The sampling was conducted by scrubbing manually the cooling side of two facing plates and collecting the removed deposits in a clean container. The plates and the scrubber were rinsed with 2.5–5 L of distilled water which was also collected in the clean container. Since each pair of plates were facing and in contact with the same water (Fig. 2B), deposits were collected in the same container for both plates. An increased number of plates were sampled in the first part of the HX (i.e. plate no. 1, the entry point of the fluid), with five pairs in the first quarter of the HX and two pairs in the last quarter. Higher deposition rate was expected at the inlet. Images were captured in-situ using a portable wireless microscope 50-500X 8-LED USB Digital Microscope to ensure that all organic and loose deposits were removed from the plates.

Samples were stored at 4 °C until further analysis (total solids (TS), total fixed solids (TFS), total volatile solids (TVS), metals concentration, and X-ray diffraction (XRD)). Total and fixed solids were measured in triplicates on a volume of 30 mL for each replicate, using Method 1684 (EPA, 2001). Samples were mixed thoroughly prior to conducting the analysis.

2.3. Laboratory HX experiment

A pilot-scale setup was built to replicate the flow conditions of the full-scale system to simulate a comparable system without filtration. This is an ideal case, since there was no addition of particles and organic matter from the outside air as it would normally be the case in a cooling tower circuit. The water circulated in the pilot was collected from the full-scale circuit. The pilot setup comprised of 3 peristaltic pumps (Cole-Parmer, MasterFlex L/S, 4 channels pump head), 3 small plate heat exchangers (Wise Water, brazed plate heat exchanger, Model-BL14-10D (Derwood, MD, USA)) and a reservoir with a capacity of 50 L (Figs. 3A and 1.S). The HX had 10 plates of 20.6 cm × 7.6 cm, for a total heat transfer area of 1.35 ft^2 (0.125 m^2). The internal volume was 110 mL on the studied side of the HX. The heat exchanger plates were brazed altogether and could not be separated manually (Fig. 3B). More information about the specifications of the pilot HX and the pilot circuit are provided in Table 1S and Fig. 1S in supplemental information. Peristaltic pumps had an average flow rate of 1 L/min, scaled to have a water velocity between plates comparable to the full-scale HX (between 1.5 and 3 m/s). The aim was to achieve similar deposition patterns and environment for biofilm growth. The reservoir was filled with 34 L of purge water previously treated (anti-scalant and chlorine-based disinfectant), collected from the hospital HVAC circuit (Fig. 1) and stored at 4 °C in a cold room before use. The physicochemical characteristics of the recirculating water inside the circuit are provided in Table 2S in the supplementary information. A volume of 10 L was withdrawn from the reservoir and replaced with stored CT water twice a week, equivalent to a replacement rate of 60 % per week. The experiment was conducted from December 7, 2022, to February 1, 2023. The pilot was shut down on weekends and during the Christmas break (between Weeks 8 and 12) to replicate actual stagnation patterns. In addition, the pilot was left at room temperature, comparable to the average water temperature of 22.7 °C measured in the full-scale heat exchanger (Table 2S). The residual chlorine was below detection limit during the pilot experiment.

Biofilm sampling was carried out after 6, 8, and 12 weeks of operation. At each sampling time, a HX was removed from the pilot setup. The HX was capped to preserve the water that was in it at the time of sampling and sonicated at maximum speed for 5 min using an ultrasonic bath (Fisher-Scientific, Pittsburgh, United States). After the first sonication, the water was collected. Three more cycles of sonication were done using ultrapure water to fill the exchanger. After each sonication cycle, the water inside the HX was collected in the same container, for a total volume of 350 mL after the 4 sonication cycles. The water samples were analyzed for total solids, total dissolved solids, and total suspended solids as described in analytical methods.

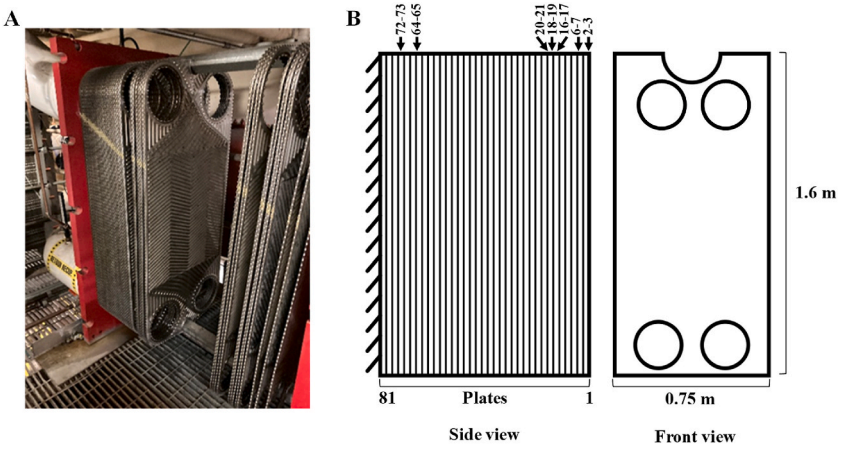

Fig. 2. 81-plate HX installed on site with 3 years of deposition (A); schematic plan of heat exchanger, sampled pairs of plates are indicated by an arrow and plate numbers (B).

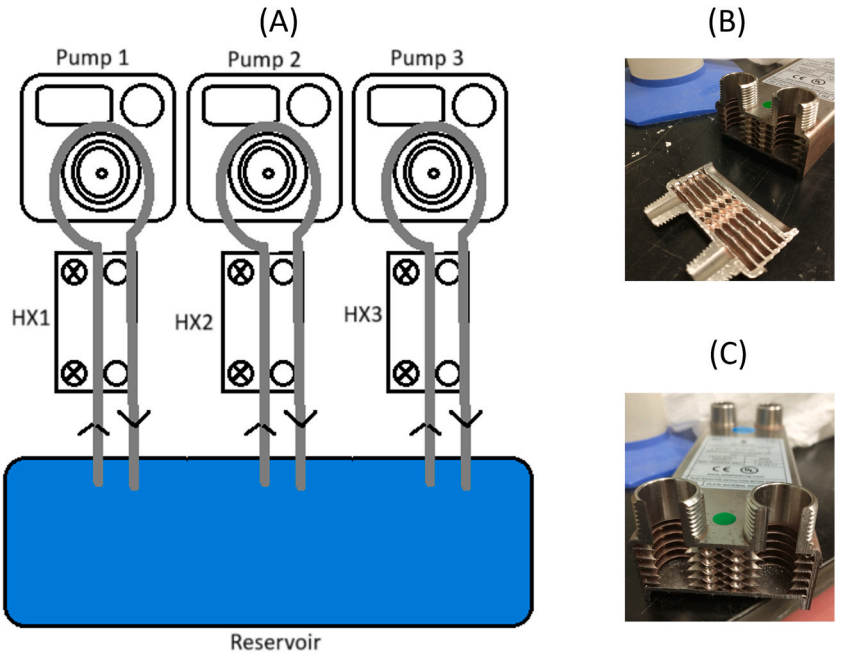

Fig. 3. Circuit diagram for pilot study on HX biofouling (A); bench top plate HX image with fused plates (B and C).

2.4. Scaling and corrosion potential indexes

Corrosion and scaling potential were evaluated using four indices [21]. The Langelier Saturation Index (LSI) can be calculated using equations (1)–(5) and is indicative of the water's ability to deposit or dissolve calcium carbonate [6]. An LSI value greater than 0.5 can lead to scaling and less than −0.5 values represent corrosion potential [6].

$$LSI = pH - pHs \tag{1}$$

Where pH is the measured water pH and pHs is the pH at saturation in calcium carbonate:

$$pHs = (9.3 + A + B) - (C + D) \tag{2}$$

$$A = (\log[\text{TDS in mg / L}] - 1)/10 \tag{3}$$

$$B = -13.12 \times \log[T(^{\circ}C) + 273] + 34.55 \tag{4}$$

$$C = \log[Ca^{2+} \text{ as } CaCO_3 \text{ in mg / L}] - 0.4 \tag{5}$$

$$D = \log[\text{alkalinity as } CaCO_3 \text{ in mg / L}] \tag{6}$$

The Pukorius scaling index (PSI) is an indicator of the likelihood of scale formation in water, focusing on the relationship between saturation state and the scaling potential [22]. It is calculated using equations (2)–(8).

$$PSI = 2\,pHs - pHeq \tag{7}$$

$$pHeq = 1.465 \times \log 10[\text{alkalinity as } CaCO_3 \text{ in mg / L}] + 4.54 \tag{8}$$

A PSI value of 5.5–7.5 is desirable. Values below 5.5 can lead to scale formation and values greater than 7.5 can result in corrosion [22]. Finally, the Larson-Skold (LR) Index is calculated using equation (9) and incorporates the effect of sulfate, chloride, and bicarbonate concentrations.

Bicarbonate concentration is assumed to be equal to alkalinity for pH between 6.5 and 9 [23].

Table 2
Scaling and corrosion indices at municipal and purge point of the circuit (calculated from water quality data from 12-month monitoring prior to cleaning, n = 17).

Indices	Desirable range	Municipal water average		Purge water average	
LSI	−0.5 to +0.5	−0.78 ± 0.5	Corrosive	0.56 ± 0.4	Low risk
PSI	5.5 to 7.5	11.08 ± 0.4	Corrosive	10.05 ± 0.5	Corrosive
LR	0.8 to 1.2	0.83 ± 0.2	Low risk	0.88 ± 0.2	Low risk

$$LR = \left(2 \text{ x } \left[SO_4^{2-}\right] + \left[Cl^-\right]\right) \ / \ \left[HCO_3^-\right] + 2 \text{ x } \left[CO_3^{2-}\right] \quad (9)$$

3. Results and discussion

3.1. Corrosion index analysis

First, average scaling and corrosion indices were calculated for municipal and cooling tower water in the studied system (Table 2). According to the LSI and PSI calculated in municipal water, it is considered corrosive. However, the addition of anti-scalant lowered the risk in the cooling tower system (Table 2). Overall, the water has a low scale formation potential, reducing fouling of the HX surfaces. The water quality was attributed to routine maintenance, continuous side stream filtration, and effective addition of anti-scaling and anti-corrosive agents in the cooling tower water system.

3.2. Biofouling development in the in-situ HX with side-stream filtration vs. pilot HX without side-stream filtration

A visual examination of the in-situ HX plates exposed to the CT water was performed before (Fig. 4a) and after cleaning (Fig. 4b). Before cleaning, the depositions appeared to be mainly organic and located on the upper part of the HX plates. All the organic and loose deposits were scrubbed, washed, and collected. White deposits associated with scaling located on the edges of the plates could not be collected through manual scrubbing. Plates were further cleaned by mechanical scrubbing and pressure washing.

Fig. 5A shows the results of total fixed solids (TFS) and total volatile solids (TVS) analysis on the samples in-situ HX plates after 3 years of operation with side-stream filtration and Fig. 5B shows the TFS, TVS, and polysaccharides analysis results for the pilot HX after 6, 8, and 12 weeks of operation without side-stream filtration. The presence of biofilm in the full-scale HX was estimated by measuring the concentration of TVS. The TVS represents an approximation of the amount of organic matter present in the total solids fraction [24], which includes polysaccharides along with other organic materials like proteins and lipids. The polysaccharides concentration represents a fraction of the organic mater in biofilm, estimated to 10–20 % once the water is removed [25]. In the pilot HX (Fig. 5B), the ratio of polysaccharides to TVS varied between 7 and 11 % in the three samples. In the in-site HX (Fig. 5A), a maximum TVS concentration of 77 μg/cm^2 was observed on the initial plates (2–3) of the HX. The concentration appears stable through the rest of the plates, except for plates 20–21. This lower value could be in part due to the variability associated with the analytical method (up to 10 % standard deviation) and to the sampling method. The lack of measurements between plates 20–21 and 64–65 does not allow to conclude on the biofouling in the middle section of the HX. The observed accumulation is notably lower compared to the previous studies. Ilhan-Sungur and Çotuk [11] reported an accumulation of 85.4 μg/cm^2 of carbohydrates after only 10 months of operation in a pilot-scale system without side stream filtration. Similarly, Pinel et al. [26] reported a polysaccharides concentrations of 140.4–365.0 μg/cm^2 after only 40 days of operation in a system without side stream filtration.

In the pilot HX (Fig. 5B), the concentration of TVS was 50 μg/cm^2 after 6 weeks and 8 weeks, and increased up to 90 μg/cm^2 after the 12th week. The polysaccharide concentrations gradually increased from 3.4 μg/cm^2 after 6 weeks to 6.5 μg/cm^2 after 12 weeks of pilot operation without filtration.

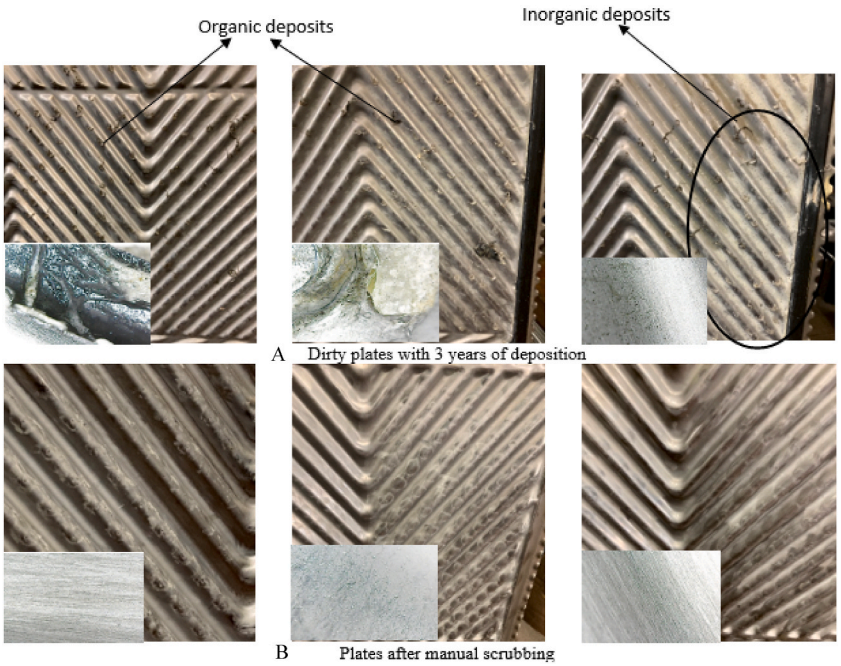

Fig. 4. Selected plates before cleaning (A), clean plates after mechanical scrubbing and pressure washing (B); Pictures on the bottom left of each figure are the 500X microscopic images of deposits on the HX plates.

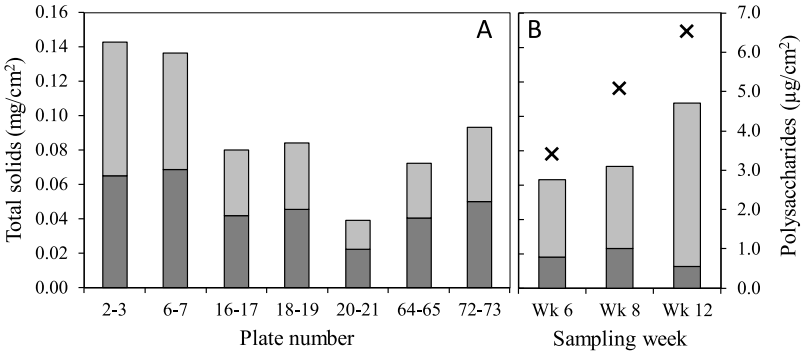

Fig. 5. Total fixed (dark gray) and volatile (light gray) solids per surface area in the full-scale heat exchanger (A) and in the pilot heat exchanger (B). Both panels share the same scale for solids. Polysaccharide concentrations (**X**) measured in the pilot heat exchanger are shown (B).

Comparing the TVS accumulation in the in-situ HX with the pilot HX and with previous studies shows that the implementation of crossflow microsand filtration significantly mitigates particle accumulation on the HX plates over time. The use of crossflow microsand filtration can help stabilize fouling to minimal levels even after a prolonged 3-year operation period without cleaning of the HX. There are however several operational or environmental factors such as air quality, type of pollutants and temperature, that can also affect the fouling in a system. Water quality can have a great impact and the lack of information on water quality in other studies where polysaccharides were evaluated prevents a true comparison.

3.3. *Composition analysis of the in-situ HX deposits*

To better understand the composition of the fixed solids on the full-scale HX plates, an XRD analysis was conducted on a composite sample prepared from solids collected from all the sampled plates (Fig. 6). The most prevalent species identified was calcium carbonate or calcite. The presence of calcium carbonate precipitates is associated with the water hardness and is impacted by water temperature and pH [27]. The accumulation of calcium carbonate on surfaces exposed to drinking water with medium to high hardness levels [28] is frequent. Other metals like magnesium and silica were also detected in carbonate and oxide form respectively. The presence of silicon in the municipal water supplies may have contributed to the progressive accumulation of silica inside the system [29].

Fig. 7 presents the result for the metal concentrations in the in-situ HX plates. Nearly all metals show a consistent pattern when analyzed plate by plate, with the maximum deposition observed on the first plate, followed by a decreasing trend that stabilizes in the middle plates before increasing again toward the end plates. The average concentrations of aluminum (0.14 µg/cm^2), silicon (0.2 µg/cm^2), iron (0.5 µg/cm^2), and copper (0.38 µg/cm^2) were lower compared to the average concentrations of Mg (0.84 µg/cm^2) and Ca (12.54 µg/cm^2). Calcium and magnesium are the multivalent cations contributing to the water hardness. In Montreal municipal water, mean concentrations of calcium and magnesium are respectively 30 mg/L and 8 mg/L, compared to concentrations below 1 mg/L for the other metal ions measured [30]. It is hypothesized that the higher concentration of calcium and magnesium in the makeup water lead to higher accumulation in the biofilm and deposits on the HX plates. The results in the first part of the HX are consistent with

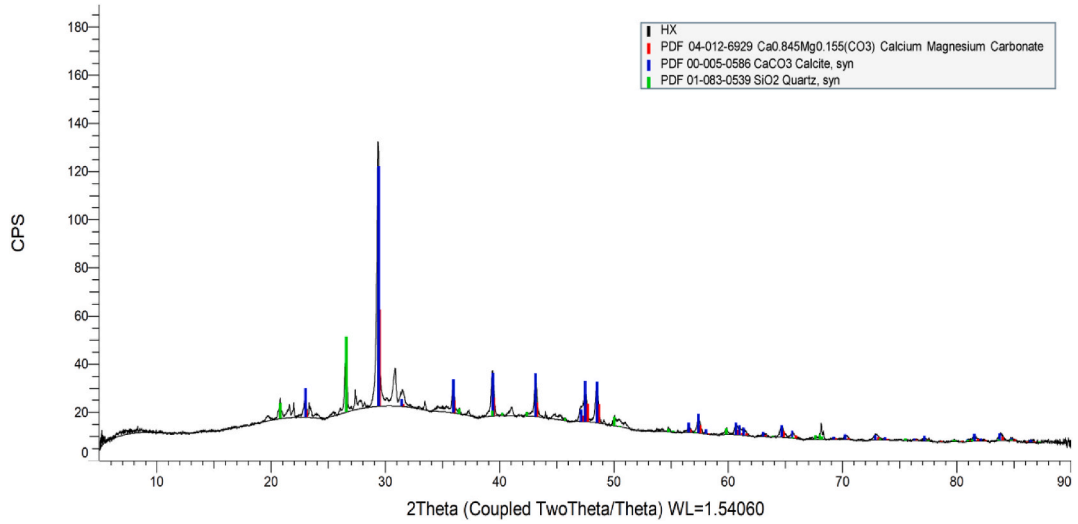

Fig. 6. XRD analysis result of solids recovered from the in-site HX plates after 3 years of deposition.

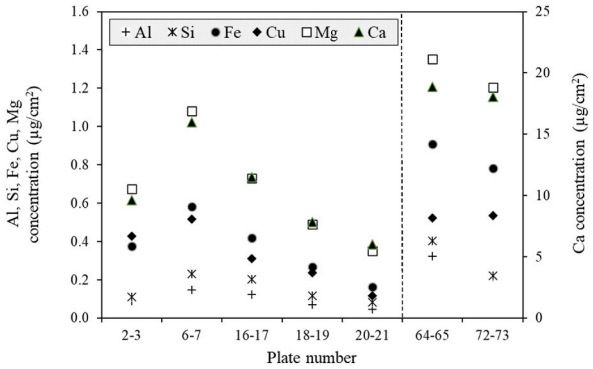

Fig. 7. Metal concentrations on sampled in-situ HX plates. The dotted line represents the separation between the plates sampled in the first quarter of the HX and the plates samples in the last quarter.

findings from the previous studies by Gao et al. [13] and Xu et al. [31], who attempted to illustrate time-based deposition of metals in three phases: introduction, deposition, and stabilization. Increased metal depositions at the end plates is due to the rise in exit pressure and increased turbulence just before the metal leaves the HX [32]. Higher deposition in the first HX plates can be due to shift in flow distribution, strong turbulence and temperature differential which enhanced precipitation of dissolved ions [32].

The TFS composition was extrapolated using the metal composition and the XRD analysis. Calcium carbonate was the most abundant species constituting 65.7 % of the TFS followed by magnesium carbonate accounting for 6.1 % of the TFS and silica making up 0.9 % of the TFS. Collectively, these three species are estimated to constitute approximately 72.7 % of the total non-volatile or total fixed solid deposition.

3.4. Study limitations

This study compared the efficiency of a crossflow microsand filtration unit in an industrial full-scale heat exchanger with a lab-scale heat exchanger. Although the operating conditions were similar by using the same CT water, HX material (both stainless steel), temperature, water velocity and stagnation patterns, there were differences in chlorine concentrations between the pilot and in-situ HX. Furthermore, the water from pilot installation was in a closed loop without an exchange with the outside air. Mimicking the outside air exchange that would happen in an open cooling tower located on a roof was a challenge and could not be undertaken. The absence of chlorine in the water could enable more bacterial growth in between water changes, leading to increased biofouling, while the closed loop operation would reduce the solids entering the systems, therefore reducing the fouling potential on the surfaces. For example, the concentration of pollen varies over time during the season and from one year to the next, making it difficult to simulate at pilot scale. Consequently, the fouling observed in the pilot could be over or underestimated. Despite these differences, the pilot scale study was helpful to qualitatively analyze the fouling potential. However, the conditions of the test (i.e., scale, flowrate, duration) should be considered when comparing results and one should avoid using the absolute values.

4. Conclusion

The main objective of this paper was to address the existing research gap in the direct fouling estimation of onsite industrial-scale heat exchangers. Two units were compared, an in-situ HX with a side stream filtration unit and a pilot HX unit operating with the same CT water and similar operating conditions as the in-situ unit but without the side stream filtration. The study key findings are summarized as follow:

- Both municipal and purge water (coming from cooling tower) exhibited low scaling potential, measured by LSI, PI, and LR indices. This was attributed to continuous side stream filtration as well as good maintenance and the use of anti-scaling and anti-corrosive agents.
- Magnesium and calcium emerge as the predominant inorganic deposits on the HX plates, with an average long-term accumulation of 12.54 µg/cm^2 and 0.84 µg/cm^2, respectively.
- The highest concentrations of TS (143 µg/cm^2), and TVS (77 µg/cm^2) are observed at the heat exchanger entrance, gradually decreasing and levelling out.
- Metal concentrations on the sampled HX plates exhibit a consistent pattern, with a slight increase in the end plates. This increase can be attributed to the exit pressure rise and strong turbulence before the fluid exits the heat exchanger.
- The in-situ HX with side stream filtration exhibited very low deposition after 3 years of continuous operation (without cleaning) with an average TS of 93 µg/cm^2 and an average TVS of 45 µg/cm^2. The low TVS values are indicative of low polysaccharides deposition and hence, low biofouling potential.
- Without side stream filtration, the pilot maximum TS deposition reached 110 µg/cm^2 and the maximum TVS reached 90 µg/cm^2 after only 12 weeks of operation.
- Comparing the in-situ HX deposits with the pilot HX suggest the role of side stream filtration in reducing particle deposition and, consequently, decreasing biofouling potential.

Crossflow microsand filtration is a promising avenue to control fouling and improve system's energetic performance in a sustainable way. The reduction in fouling on heat exchange surfaces can contribute in improving the building energetic performance by increasing heat transfer capacity. Future research should focus on quantifying the impact of side stream filtration on the operational efficiency and energy savings of HVAC units.

CRediT authorship contribution statement

Vaishali Ashok: Writing – original draft, Methodology, Investigation, Formal analysis, Conceptualization. **Faezeh Absalan:** Writing – review & editing, Visualization, Validation, Formal analysis. **Alain Silverwood:** Writing – review & editing, Resources, Methodology, Conceptualization. **Etienne Robert:** Writing – review & editing, Validation, Conceptualization. **Dominique Claveau-Mallet:** Writing – review & editing, Validation, Supervision, Resources, Methodology, Investigation, Conceptualization. **Emilie Bédard:** Writing – review & editing, Validation, Supervision, Resources, Project administration, Methodology, Investigation, Funding acquisition, Formal analysis, Conceptualization.

Declaration of competing interest

The authors declare the following financial interests/personal relationships which may be considered as potential competing interests:

Emilie Bedard reports financial support was provided by Mitacs Canada. Emilie Bedard reports financial support was provided by Evoqua Water Technologies LLC Montreal. The co-author Alain Silverwood is an employee of Xylem Water Solutions and Water Technology (formerly Evoqua Water). He provided his help during the onsite sampling but did not perform any of the laboratory or data analysis. If there are other authors, they declare that they have no known competing financial interests or personal relationships that could have appeared to influence the work reported in this paper.

Data availability

Data will be made available on request.

Acknowledgements

This work was supported by a research grant from MITACS – Accelerate program, Canada (IT27607), in partnership with Evoqua Water Technologies LLC. A.S. is an employee of Evoqua Water Technologies LLC, the company sponsoring the research project and providing the device. We thank the staff from the study site for sharing data, site information and access to site premises to carry out this study, and Olivier Godfroy and Ziyed Sahlia for their help with sampling and pilot operation.

NOMENCLATURE

CT	cooling tower
Gpm	gallons per minute
HX	heat exchanger
HVAC	Heating, ventilation and air-conditioning
TS	Total solid
TSS	Total suspended solid
TFS	Total fixed solid

Appendix A. Supplementary data

Supplementary data to this article can be found online at https://doi.org/10.1016/j.jobe.2024.110167.

References

[1] L. Cremaschi, J.D. Spitler, E. Lim, A. Ramesh, Waterside fouling performance in brazed-plate-type condensers for cooling tower applications, HVAC R Res. 17 (2) (2011) 198–217.
[2] CPD, Canadian Patents Database, Government of Canada, 2024. https://www.ic.gc.ca/opic-cipo/cpd/eng/search/basic.html?wt_src=cipo-patent-main.
[3] S. García, A. Trueba, Inverse Heat Conduction and Heat Exchangers, IntechOpen, 2019, pp. 1–26.
[4] J. Xu, J. Zhao, Y. Jia, Experimental study on the scale inhibition effect of the alternating electromagnetic field on CaCO3 fouling on the heat exchanger surface in different circulating cooling water conditions, Int. J. Therm. Sci. 192 (2023) 108388.
[5] K. Shaikh, S.N. Kazi, M.N.M. Zubir, B. Abd Razak, K. Wong, Y.H. Wong, W.A. Khan, S. Abdullah, M.S. Alam, Investigation of zirconium (Zr) coated heat exchanger surface for the enhancement of heat transfer and retardation of mineral fouling, J. Taiwan Inst. Chem. Eng. 153 (2023) 105246.
[6] L. Duvivier, Treatment of Cooling Water, Springer, 2009, p. 191.
[7] X. Dong, X. Zhai, J. Yang, F. Guan, Y. Zhang, J. Duan, B. Hou, Two metabolic stages of SRB strain Desulfovibrio bizertensis affecting corrosion mechanism of carbon steel Q235, Corrosion Communications 10 (2023) 56–68.
[8] H. Müller-Steinhagen, M. Malayeri, A. Watkinson, Heat Exchanger Fouling: Mitigation and Cleaning Strategies, Taylor & Francis, 2011, pp. 189–196.

[9] E. Daamen, J. Wouters, J. Savelkoul, Side stream biofiltration for improved biofouling control in cooling water systems, Water Sci. Technol. 41 (4–5) (2000) 445–451.
[10] X. Duan, J. Williamson, K. McMordie, Side stream filtration for cooling towers. Federal Energy Management Program, US Department of Energy, 2012.
[11] E. Ilhan-Sungur, A. Çotuk, Microbial corrosion of galvanized steel in a simulated recirculating cooling tower system, Corrosion Sci. 52 (1) (2010) 161–171.
[12] M.S. AlSalhi, S. Devanesan, A. Rajasekar, S. Kokilaramani, Characterization of plants and seaweeds based corrosion inhibitors against microbially influenced corrosion in a cooling tower water environment, Arab. J. Chem. 16 (3) (2023).
[13] R. Gao, C. Shen, X. Wang, Y. Yao, Experimental study on the fouling and heat transfer characteristics of enhanced tubes used in a cooling tower water system with the actual water quality, Int. J. Therm. Sci. 181 (2022) 107777.
[14] I. Pinel, R. Biskauskaite, E. Pal'ova, H. Vrouwenvelder, M. van Loosdrecht, Assessment of the impact of temperature on biofilm composition with a laboratory heat exchanger module, Microorganisms 9 (6) (2021).
[15] P.S. Murthy, R. Venkatesan, K.V.K. Nair, M. Ravindran, Biofilm control for plate heat exchangers using surface seawater from the open ocean for the OTEC power plant, Int. Biodeterior. Biodegrad. 53 (2) (2004) 133–140.
[16] K.P.H. Meesters, J.W. Van Groenestijn, J. Gerritse, Biofouling reduction in recirculating cooling systems through biofiltration of process water, Water Res. 37 (3) (2003) 525–532.
[17] M. Soliman, F. Eljack, M.-K. Kazi, F. Almomani, E. Ahmed, Z. El Jack, Treatment technologies for cooling water blowdown: a critical review, Sustainability 14 (1) (2021) 376.
[18] A.-B. Mohammed, A.K.S. Raju, J. Lee, Y. Oh, S. Jeong, Non-chemical biofouling mitigation systems for seawater cooling tower using granular activated carbon biofiltration and ultrafiltration, J. Environ. Chem. Eng. 9 (6) (2021) 106784.
[19] J. Narenkumar, P. Elumalai, S. Subashchandrabose, M. Megharaj, R. Balagurunathan, K. Murugan, A. Rajasekar, Role of 2-mercaptopyridine on control of microbial influenced corrosion of copper CW024A metal in cooling water system, Chemosphere 222 (2019) 611–618.
[20] P. Kapustenko, J.J. Klemeš, O. Arsenyeva, Plate heat exchangers fouling mitigation effects in heating of water solutions: a review, Renew. Sustain. Energy Rev. 179 (2023).
[21] M.K. Zia, H.N. Bhatti, I.A. Bhatti, R. Nawaz, A pHs equation for calcium carbonate scale prediction in cooling water systems, J. Chem. Soc. Pakistan 30 (2008) 182–185.
[22] E. Hoseinzadeh, A. Yusefzadeh, N. Rahimi, H. Khorsandi, Evaluation of Corrosion and Scaling Potential of a Water Treatment Plant, 2013, pp. 41–47.
[23] H. Khorsandi, A. Mohammadi, S. Karimzadeh, J. Khorsandi, Evaluation of corrosion and scaling potential in rural water distribution network of Urmia, Iran, Desalination Water Treat. 57 (23) (2016) 10585–10592.
[24] R. Baird, L. Bridgewater, Standard Methods for the Examination of Water and Wastewater, 23rd edition, 2017. Washington, DC.
[25] M.A. Rather, K. Gupta, M. Mandal, Microbial biofilm: formation, architecture, antibiotic resistance, and control strategies, Braz. J. Microbiol. 52 (4) (2021) 1701–1718.
[26] I. Pinel, R. Biškauskaitė, E. Pal'ová, H. Vrouwenvelder, M. van Loosdrecht, Assessment of the impact of temperature on biofilm composition with a laboratory heat exchanger module, Microorganisms 9 (6) (2021) 1185.
[27] J. MacAdam, S.A. Parsons, Calcium carbonate scale formation and control, Rev. Environ. Sci. Biotechnol. 3 (2) (2004) 159–169.
[28] Heatlh Canada, Guidelines for Canadian Drinking Water Quality: Guideline Technical Document – Hardness, 1979, p. 4.
[29] P. Besevic, S.M. Clarke, G. Kawaley, D.I. Wilson, Effect of silica on deposition and ageing of calcium carbonate fouling layers, Heat exchanger fouling and cleaning (2017) 58–66.
[30] Ville de Montréal, Drinking Water Quality Annual Testing Reports, 2023.
[31] Z. Xu, A. Sun, Z. Han, X. Yu, Y. Zhang, Simulation of particle deposition in a plate-fin heat exchanger using a particle deposition model with a random function method, Powder Technol. 355 (2019) 145–156.
[32] B. Zohuri, Compact Heat Exchangers-Selection, Application, Design and Evaluation, Springer, USA, 2017.
[33] A. Singh, K.R. Ansari, M.A. Quraishi, Inhibition effect of natural polysaccharide composite on hydrogen evolution and P110 steel corrosion in 3.5 wt% NaCl solution saturated with CO2: combination of experimental and surface analysis, Int. J. Hydrogen Energy 45 (46) (2020) 25398–25408.
[34] W. Zhang, Y.-C. Wu, H.-J. Li, Apostichopus japonicus polysaccharide as efficient sustainable inhibitor for mild steel against hydrochloric acid corrosion, J. Mol. Liq. 321 (2021).
[35] A. Zaza, E.G. Bennouna, A. Iranzo, Y. El Hammami, Identifying fouling mechanism in a novel hybrid cooling tower's bundles: application in concentrated solar power (CSP) plant, Int. Commun. Heat Mass Tran. 149 (2023).